Chapter 1

Introduction

1.1 Starburst galaxies

Shortly after the Big Bang around 13.7 billion years ago, all elementary particles, which later formed hydrogen and helium, were mixed together in a hot, dense, primordial soup. This soup was distributed *almost* homogeneously over the entire Universe, with only very small fluctuations. These were discovered by NASA's Cosmic Background Explorer (Smoot et al. 1992; Mather et al. 1999) and later mapped with more precision by the Wilkinson Microwave Anisotropy Probe (Bennett et al. 2003). In the course of the evolution of the Universe, these tiny density fluctuations grew bigger and bigger, resulting in a filamentary structure made up out of dense regions and voids (Springel et al. 2006). In the dense regions galaxies were formed, separated by large areas of 'nothing', the voids, where little baryonic matter can be found.

At first glance most galaxies in the local Universe seem to live in relative isolation. However, upon closer inspection galaxies tend to cluster together in the denser regions, and interactions with neighbours are found to be quite common. Our own galaxy, for example, swallowed several small companions in the past, and it even shows cannibal behaviour at this moment, absorbing the Sagittarius Dwarf galaxy (Ibata et al. 1994). Many galaxies show signs of recent or ongoing merging. These interactions supply fresh fuel for star formation in the form of large quantities of gas and dust. Furthermore, collisions with massive neighbours significantly disrupt the galaxy's gravitational potential, causing gas to pile up and form stars in very energetic bursts (Schweizer 2005). These objects are called starburst galaxies when the star formation rate is so high, that it would exhaust the gas reservoir in much less than a Hubble Time (Larson & Tinsley 1978; Weedman et al. 1981).

Interactions are the most important, but not the only possible trigger of starbursts. Vigorous star formation can be initiated by inward gas flows in barred galaxies, or by spontaneous global gravitational instability in dwarf galaxies as well. During the powerful bursts the star formation rate can be as high as several hundred solar masses per year, and star formation in star clusters seems to be an important mode of star formation (as opposed to the creation of a diffuse field star population, Meurer et al. 1995).

It is clear that starbursts, although relatively short-lived, are an important phase in galaxy evolution. In a short time, much of the galaxy's gas reservoir is turned into stars, rejuvenating its stellar content. In the local Universe starburst galaxies are responsible for approximately a quarter of all star formation (Heckman 1997), and evidence exists that star formation in burst mode is increasingly important if we look back in time into

the early Universe. SCUBA submillimeter (submm) data indicate that the activity of starbursting galaxies increases by a factor of 100 between the present epoch and the universe at a redshift of 3 (Blain et al. 1999). This enhanced star formation at high redshift is due to the more frequent occurence of merging events as well as the fact that bursts last longer on average. Detailed knowledge of local starburst galaxies can thus help to understand the star formation history of the Universe.

Apart from being crucial in galaxy evolution, starbursts are also very useful objects for the study of the process of star formation. In a period of only several million years, numerous massive, bright star clusters are formed. This rich collection of young star clusters forms an ideal laboratory to study the mechanisms that drive the formation of massive stars and stellar populations, and the properties of the environment in which this process takes place.

It has long been understood that starbursts happen in regions with large amounts of gas. However, the exact trigger of the star formation has not yet been firmly established. Several different models try to explain the onset of the vigorous bursts of star formation. One of these is the gravitational instability model, in which star formation begins spontaneously after enough energy has dissipated from the molecular clouds and the clouds contract due to self-gravity (Toomre 1964; Quirk 1972; Larson 1988; Kennicutt 1989, 1998; Elmegreen 1994). Another model assumes that pre-existing clouds are compressed in a high-pressure environment (Jog & Solomon 1992), increasing the density to high enough values for star formation to take place. In a third model the required high densities are reached in cloud-cloud collisions (Wyse 1986; Wyse & Silk 1989; Silk 1997; Tan 2000). In addition to these mechanisms, the process of triggered star formation is thought to be very important in starburst galaxies. When outflows due to stellar winds and supernova explosions of the first generation of stars compress the surrounding interstellar medium (ISM), the formation of following generations of stellar populations is triggered in nearby molecular clouds (Elmegreen & Lada 1977). Triggered star formation can be identified in the form of age gradients within the starburst region. High-velocity cloud-cloud collisions would leave their fingerprints in the form of high cluster-to-cluster velocity dispersions. The gravitational instability and the compression model are harder to distinguish, since they both do not leave very clear marks (except for characteristic sizes and masses for the individual star-forming regions).

1.2 Observational characteristics of starburst galaxies?

Starbursts can take place at various locations in a galaxy. Most common are bursts of star formation in (a ring around) the nucleus of a large (barred) spiral galaxy. With gas moving inward along the spiral arms, or slowing down due to the torque it experiences from the galaxy's bar, large amounts of gas can accumulate at these central regions. Active star formation can take place in the disk as well, or in case of a major merger, all over the system of colliding galaxies. In highly perturbed galaxies, bright young star clusters are also observed far from the center, in the tidal features ejected from the galaxy during the interaction.

These sites of active star formation host numerous massive, bright star clusters. In

general, the youngest of these clusters are still heavily embedded in their natal clouds, resulting in very red cluster colors due to large extinction. With increasing age, the molecular cloud around the cluster disperses and/or is blown away by stellar winds and supernovae, revealing bright stellar populations with very blue colors, since the integrated light is still dominated by very massive and hot stars. When these most massive stars evolve off the main sequence and dissapear, the cluster becomes increasingly red as cooler stars become more important. There are indications that most of the clusters formed in these starburst events are not gravitationally bound and disperse on a typical timescale of 10 Myr. This process, called infant mortality, is observed in various starburst galaxies (Lada & Lada 2003; Mengel et al 2005; Fall et al. 2005; Bastian et al. 2006; Pellerin et al. 2007; Gilbert & Graham 2007). However, older clusters up to several hundred Myrs are identified in (post-)starburst galaxies as well (for example in the Antennae, Whitmore et al. 1999). These clusters are possibly the precursors of the old, gas-poor, very massive globular clusters observed in the Milky Way.

Stellar winds and far-ultraviolet radiation from the cluster's massive O and B stars clear the direct environment of the cluster by sweeping away most of the dust. Most gas in these so-called H II regions is ionized, and strong emission lines can be observed; hydrogen and helium recombination lines as well as fine-structure lines of various species. Further out from the star cluster, where only softer radiation penetrates, photodissociation regions (PDRs) can be found. In these regions, dust, polycyclic aromatic hydrocarbons (PAHs), CO and H_2 molecules are mostly left intact, and are excited or heated by the more energetic photons that reach the PDR. This results in various spectral features; a rising continuum longwards of 15 μm characteristic for thermal emission from heated dust, various rotational (mid-infrared) and ro-vibrational (near-infrared) H_2 emission lines, and broad emission bands associated with the PAHs.

In the violent environments around these active star-forming regions, photoionization is not the only important excitation mechanism. Stellar winds and supernovae sweep up the ISM surrounding the star cluster, causing shocks in which the excitation of various species and the grain/molecule formation and destruction balance is affected.

1.3 This thesis

In this thesis we focus on the youngest stellar populations formed during the most recent burst of star formation. The questions addressed are the following:

- What are the properties of the (super) star clusters; what are their masses, sizes, upper mass cutoffs; what is the star formation rate in these star-forming regions? *Chapters 2, 4, 5, and 6*
- What are the properties of the medium in which the clusters are formed; what is the spatial distribution of the ISM; what is the density of the ionized and molecular gas; what is the metallicity? What is the dominant excitation mechanism for the various species? *all Chapters*
- To what extent is the bright PAH emission a tracer of the star formation in starburst galaxies? *Chapters 2, 5 and 6*

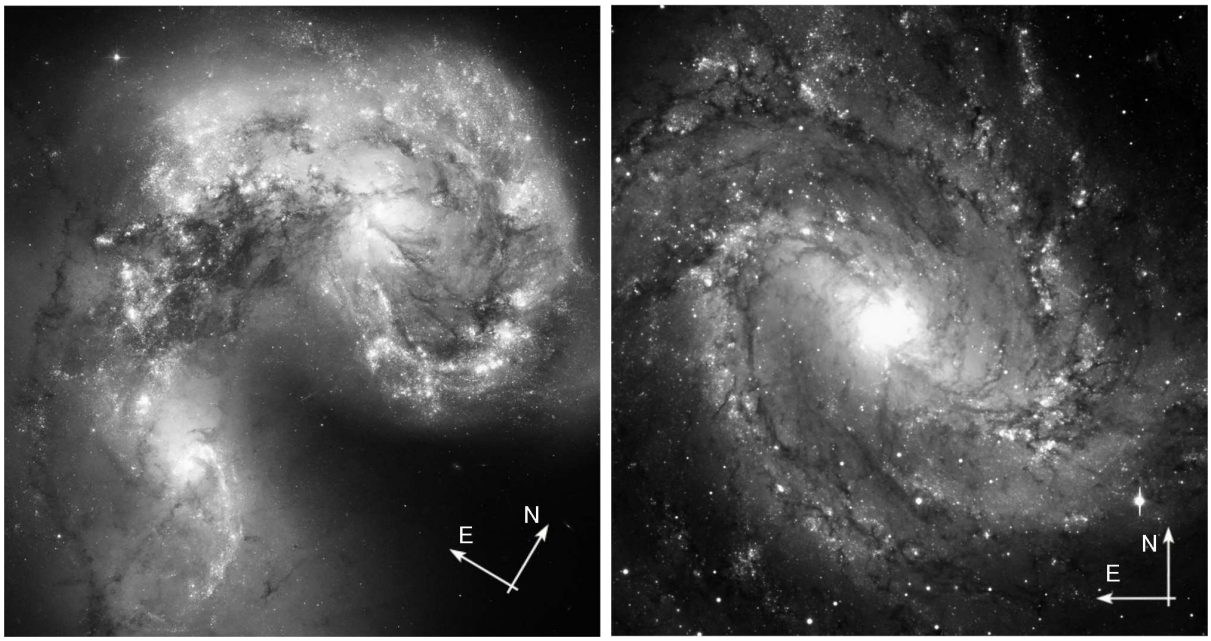

Figure 1.1 — *Left:* Optical image of the two merging spiral galaxies the Antennae (NGC 4038/4039), obtained with the Advanced Camera for Surveys at the Hubble Space Telescope (courtesy Bradley Whitmore, NASA, ESA, and the Hubble Heritage Team (STScI/AURA), ESA/Hubble Collaboration). The angular size is of this image approximately 2.1×2.3 arcmin^2 *Right:* The barred spiral M83, as observed with the visual and near UV FOcal Reducer and low dispersion Spectrograph (FORS) at the Very Large Telescope (courtesy: the FORS-Team, ESO). The field size is 7.0×7.4 arcmin^2 across the sky. Both images show a combination of several optical filters.

1.4 Objects

To address these questions, (super) star clusters and their environments are observed in two starburst galaxies, the major merger NGC 4038/4039 (the Antennae) and M83.

1.4.1 The Antennae

The Antennae galaxies, NGC 4038/4039 (Arp 244), form one of the most striking nearby examples of a major merger in action. The two long antenna-like tidal tails, which gave the system its name, span approximately 20′ along the sky, which is almost the size of the full moon. Together, the two colliding Sc spiral galaxies, form the first system in the Toomre (1977) merger sequence. The initial encounter took place approximately 210 Myr ago and simulations indicate that these two giant spirals will eventually merge into an elliptical-like galaxy (Mihos et al. 1993). The distance to the system is still under debate. Earlier estimates by Stanford et al. (1990); Wilson et al. (2000); Gao et al. (2001) found 20 - 21 Mpc, and Whitmore et al. (1999) determined 19.2 Mpc. Using the Wide-Field Planetary Camera 2 on the Hubble Space Telescope to study the stellar populations at the tip of the Southern tail, Saviane et al (2004) observed the tip of the red giant branch and determined a distance of only 13.8 ± 1.7 Mpc. Throughout this thesis we will adopt the distance of 21 Mpc (Stanford et al. 1990), which is most commonly used in the literature. The Antennae's infrared luminosity between 1 – 1000 μmwas measured by the Infrared Space Observatory (ISO) to be $L_{FIR} = 6.4 \cdot 10^{10} \mathrm{L}_{\odot}$(Klaas et al.

1997), just below the treshold of luminous infrared galaxies of $10^{11}L_{\odot}$.

Since the beginning of the interaction the system has gone through several episodes of violent star formation of which the last one is probably still ongoing (Vigroux et al. 1996). The resulting (super) star clusters and the surrounding ISM have been studied extensively throughout the electromagnetic spectrum (Zezas et al. 2002; Baldi et al. 2006; Clark et al. 2007; Whitmore & Schweizer 1995; Whitmore et al. 1999; Whitmore & Zhang 2002; Whitmore et al. 2005; Brandl et al. 2005; Gilbert et al 2000; Gilbert & Graham 2007; Mengel et al 2001; Mengel et al. 2002; de La Fuente Marcos & de La Fuente Marcos 2006; Haas et al. 2005; Wang et al. 2004; Zhang, Fall & Whitmore 2001; Vigroux et al. 1996; Mirabel et al 1998; Snijders et al 2006, 2007; Stanford et al. 1990; Wilson et al. 2000; Gao et al. 2001; Schulz et al. 2007). Most of the clusters are young, bright, intrinsically very blue stellar populations, but clusters with an age of several hundreds Myrs, probably formed during the first fly-by, can be identified as well (Whitmore et al. 1999). Statistical studies of the age distribution of the whole star cluster population indicate that most massive clusters dissolve on a timescale of the order of 10 Myr (Mengel et al 2005; Fall et al. 2005; Gilbert & Graham 2007).

Radio and mid-infrared observations showed that the region between the two spiral galaxies (the overlap region) hosts spectacular obscured star formation. The brightest mid-infrared component produces 15% of the total 15 μm luminosity of the entire system (Mirabel et al. 1998; Hummel & Van der Hulst 1986). This star-forming region is covered by a prominent dustlane and may be associated with a faint, red source in the Hubble Space Telescope (HST) images (No. 80 of Whitmore & Schweizer 1995), illustrating how optical data alone are insufficient to identify and study the youngest star-forming regions.

1.4.2 M83

At 4.5 Mpc (Cepheid distance, Thim et al 2003), M83 (NGC 5236) is the nearest large barred spiral. M83 lives in the Hydra group of galaxies and deep HI images show evidence for tidal arms in the outer parts of the spiral, indicating that the spiral is interacting with its close neighbour, NGC 5253 (Park et al 2001; Huchtmeier & Bohnenstengel 1981). Both NGC 5253 and the nucleus of M83 undergo a vigorous burst of star formation (Calzetti et al 1997, 1999; Tremonti et al 2001), but since the last close passage between these two galaxies took place 1 – 2 Gyr ago (van den Bergh 1980; Caldwell & Phillips 1989), it is unclear whether these starbursts are directly triggered by the interaction.

The morphology of the central 300 pc around the nucleus of M83 is extremely complex (Gallais et al 1991; Elmegreen et al 1998; Thatte et al 2000). Harris et al (2001) identified around 400 star clusters from HST images. As is frequently observed in barred spirals, most of these hotspots seem to be oriented along a circumnuclear ring, which is probably close to the Inner Lindblad Resonance (Elmegreen et al 1998). However, the whole nuclear region is affected by patchy, and often large, column densities of obscuring dust, hiding part of the starburst ring from view. This complicates the detailed understanding of the morphology in general. Relative to the optically defined nucleus, the most prominent source in the mid-infrared and radio, which corresponds to the most active region of star formation, is offset by $\sim$ 4.″4 to the west ($\sim$100 pc in

projection at a distance of 4.5 Mpc; at this distance 1″ corresponds to 22.5 pc), at the edge of the starburst ring (Telesco 1988; Gallais et al 1991, and this work).

1.5 Observations

Since the earliest stages of massive star formation are generally heavily enshrouded by dust, observations at infrared wavelengths are essential. In such observations, the youngest stellar populations are visible and various diagnostic features are available to study both the properties of the associated ISM and the stellar population. While near-infrared data are occasionally used in this thesis (mainly Chapter 4), ground- and space-based mid-infrared observations form the major component of the study presented in the following Chapters. For this reason the main focus of this Section will be the mid-infrared wavelength regime.

Being less challenging due to the properties of the earth's atmosphere, near-infrared observing techniques are much more mature than those in the mid-infrared. The first large-area near-infrared survey was carried out already in 1968 (Two Micron Sky Survey; Neugebauer & Leighton 1969). Steady technological progress ever since resulted in many different near-infrared instruments, operational at telescopes all over the world, routinely observing in the J-, H-, K-, L-, and M-band (1.1 – 1.4, 1.5 – 1.8, 2.0 – 2.4, 3.0 – 4.0, and 4.6 – 5.2 μm, respectively).

Over the last decades the field of mid-infrared astronomy has received an enormous impulse from observations with space telescopes; from IRAS in the eighties, ISO in the nineties and currently from the Spitzer Space Telescope. However, as discussed by Martín-Hernández et al. (2005), the interpretation of large aperture mid-infrared observations obtained with space telescopes can be challenging, especially for extragalactic objects due to the limited spatial resolution achieved. Ground-based mid-infrared astronomy faces different challenges due to the characteristics of the earth's atmosphere, but thanks to rapid progress in detector technology, several mid-infrared instruments have become available on large ground-based observatories in the past five years. Compared to observations from space, ground-based work offers the considerable advantage of a more detailed view of the objects of interest, due to the much higher spatial resolution that can be obtained. For example, the typical size of a star-forming region is a few to a few tens of parsecs. With its 85 cm mirror, Spitzer can resolve details on a 50 parsec scale in objects out to 4 Mpc distance. With an 8 meter class telescope similar scales can be resolved out to 40 Mpc, increasing the volume that can be probed at this resolution by a factor of a thousand. Unfortunately, the atmosphere is opaque to most infrared radiation, making it impossible to access the full infrared wavelength regime from the ground. This means that we are limited to a number of specific atmospheric windows of (reasonably) good transmission; the N-band from 8 to 13 μm and the Q-band between 16.5 and 24.5 μm.

1.5.1 Ground-based

In this thesis, near-infrared data from two different instruments are used; longslit spectra from the Infrared Spectrometer And Array Camera (ISAAC, Moorwood et al 1998) and a spectral map from the Spectrograph for INtegral Field Observations in the Near

Infrared (SINFONI, Eisenhauer et al 2003; Bonnet et al 2004), both mounted at one of the 8.2 m VLT mirrors.

ISAAC offers various imaging and spectroscopic observing modes in the wavelength range of 1 – 5 μm. The instrument has two arms, one for the short wavelength (SW) observations in the J-, H-, and K-band, and the other for the 3 – 5 μm range (LW; L- and M-band). With the options of a small and an large pixel scale ($0\farcs071$ pix^{-1} and $0\farcs148$ pix^{-1}, respectively), the two 1024 $\times$ 1024 detectors result in a field of view of $73'' \times 73''$ or $152'' \times 152''$. For the SW arm a set of five broadband and sixteen narrowband filters is available, and for the LW arm one broadband and two narrowband filters can be chosen from. In addition, various polarimetric setups are offered. For spectroscopic observations, low- (R $\sim$ 500) and medium-resolution (R $\sim$ 2000 – 3000) setups are available.

SINFONI is a near-infrared (1.1 – 2.45 μm) integral field spectrograph connected to an adaptive optics module, delivering datacubes from four different gratings (J-, H-, and K-band, plus H+K). The spectral resolution is 2000, 3000, 4000, and 1500 for J-, H-, K-band, and H+K, respectively. Each band fits fully on the 2048 $\times$ 2048 detector, and the spatial scale can be chosen from $0\farcs25$, $0\farcs1$ or $0\farcs025$ per image slice, resulting in a $8'' \times 8''$, $3'' \times 3''$, or $0\farcs8 \times 0\farcs8$ field of view.

VISIR, the mid-infrared imager and spectrometer, was built by a dutch-french consortium, and saw first light in April 2004. This instrument provides diffraction-limited imaging in the N- and Q-band windows (8 – 13 μm and 16.5 – 24.5 μm, respectively), offering eleven different filters in the N-band, and an additional three in the Q-band. The longslit spectrometer can be used in low-, medium-, or high-resolution (R $\sim$ 50, R = 200 – 2000, and R = 900 – 10000, respectively). A high-resolution cross-dispersed mode (R = 1500 – 12000) is offered as well.

1.5.2 Space-based

The data presented in Chapter 5 are obtained with the Spitzer Space Telescope. This space mission is the fourth and final element in NASA's family of Great Observatories. The telescope, equipped with a 85 cm mirror, carries three cryogenically cooled instruments, the Infrared Array Camera (IRAC), the Multiband Imaging Photometer for Spitzer (MIPS), and the Infrared Spectrograph (IRS). Together, these instruments cover the wavelength range of 3.6 – 160 μm. IRAC provides images at 3.6, 4.5, 5.8, and 8.0 μm simultaneously, with a field of view of $5.2' \times 5.2'$. MIPS obtains images at longer wavelengths, at 24, 70, and 160 μm. In addition, a low-resolution spectroscopy mode for observations between 55 – 95 μm is available. With IRS, low- and medium-resolution spectra (R = 60 – 120, and R $\sim$ 600, respectively) in the range of 5.2 – 38.0 μm can be obtained.

In Chapter 2, VISIR mid-infrared ground-based imaging and N-band spectroscopy are presented, based on which the distribution of dust and PAHs around two clusters in the Antennae overlap region are discussed (see Snijders et al 2006). The first half of Chapter 3 describes our efforts to model the embedded stellar populations. In the second half of Chapter 3 the model results are used to interpret the data from Chapter 2 in combination with Q-band spectroscopy of the same sources. ISAAC near-infrared J-, H-, and K_s-band spectra of four super star clusters (including the ones from Chapter 2) are presented in Chapter 4. In this Chapter various properties of the stellar populations as well as the excitation mechanism of the detected H_2 ro-vibrational emission lines are discussed. Chapter 5 introduces space-based mid-infrared data, both high-resolution spectra of the six brightest star clusters and the merger's two nuclei (NGC 4038 and NGC 4039). In addition, low-resolution spectral maps of the entire merging system are presented.

In Chapter 6, the spatial distributions of H II regions, PAH, and H_2 emission in the complex nuclear starburst of M83 are compared in detail. This analysis is based on several mid-infrared narrowband images obtained with VISIR, plus a near-infrared H_2 line map constructed from a SINFONI K_s-band datacube.

References

Baldi, A., Raymond, J. C., Fabbiano, G., Zezas, A., Rots, A. H., Schweizer, F., King, A. R., & Ponman, T. J. 2006, ApJ 636, 158
Bastian, N. & Goodwin, S. P.,2006, MNRAS 369, 9
Bennett, C. L., et al., 2003, ApJS 148, 1
Blain, A. W., Jameson, A., Smail, I, Longair, M. S., Kneib, J.-P. & Ivison, R. J., 1999, MNRAS 309, 715
Bonnet, H. et al., 2004, The ESO Messenger 117, 17
Brandl, B. R. et al, 2005, ApJ 635, 280
Caldwell, N., & Phillips, M. M., 1989, ApJ 338, 789
Calzetti, D., Conselice, C. J., Gallagher, J. S. & Kinney, A. L.,1999, AJ 118, 797
Calzetti, D. et al., 2007, in press (arXiv:0705.3377)
Clark, D. M., et al., 2007, ApJ 658, 319
de La Fuente Marcos, R., & de La Fuente Marcos, C. 2006, MNRAS 372, 279
Eisenhauer, F. et al., 2003, SPIE 4841, 1548
Elmegreen, B. G. & Lada, C. J., 1977, ApJ 214, 725
Elmegreen, B. G., 1994, ApJ 425, L73
Elmegreen, D. Meloy, Chromey, F. R. & Warren, A. R., 1998, AJ 116, 2834
Fall, S. M., Chandar, R. & Whitmore, B. C., 2005, ApJ 631, 133
Gallais, P., Rouan, D., Lacombe, F., Tiphene, D. & Vauglin, I., 1991, A&A 243, 309
Gao, Y., Lo, K. Y., Lee, S.-W., & Lee, T.-H. 2001, ApJ 548, 172
Gilbert, A. M. et al., 2000, ApJ 533, L57
Gilbert, A. M. & Graham, J.R., 2007, ApJ in press
Haas, M., Chini, R., & Klaas, U. 2005, A&A 433, L17
] Harris, J., Calzetti, D., Gallagher, J. S., Conselice, C. J. & Smith, D. A., 2001, AJ 122, 3046
Heckman, T. M., 1997, in AIP Conf. Ser. 373, Star Formation Near and Far, eds. Holt S. S. & Mundy, L. G. (Woodbury N. Y. : AIP Press), 271
Huchtmeier, W. K. & Bohnenstengel, H.-D., 1981, A&A 100, 72
Hummel, E. & Van der Hulst, J. M., 1986, A&A 155, 151
Ibata, R. A., Gilmore, G. & Irwin, M. J., 1994, Nature 370, 194
Jog, C. J. & Solomon, P. M., 1992, ApJ 387 152
Kennicutt, R. C., Jr., 1989, ApJ 344, 685
Kennicutt, R. C., Jr., 1998, ApJ 498, 541

Klaas, U., Haas, M., Heinrichsen, I., Schulz, B., 1997, A&A 325, 21
Lada, C. J. & Lada, E. A. 2003, ARA&A 41, 57
Lagage, P. O. et al., 2004, The Messenger 117, 12
Larson, R. B. & Tinsley, B. M., 1978, ApJ 219, 46
Larson, R. B., 1988, "Galactic and Extragalactic Star Formation", eds. Pudritz , R. E. & Fich, M. (Dordrecht: Kluwer), 459
Martín-Hernández, N. L., Schaerer, D. & Sauvage. M, 2005, A&A 429, 449
Mather, J. C., Fixsen, D. J., Shafer, R. A., Mosier. C & Wilkinson, D. T., 1999, ApJL 512, 511
Mengel, S., Lehnert, M. D., Thatte, N., Tacconi-Garman, L. E. & Genzel, R., 2001, ApJ 550, 280
Mengel, S., Lehnert, M. D., Thatte, N. & Genzel, R., 2002, A&A 383, 137
Mengel, S., Lehnert, M. D., Thatte, N. & Genzel, R., 2005, A&A 443, 41
Meurer, G. R., Heckman, T. M., Leitherer, C., Kinney, A., Robert, C. & Garnett, D. R., AJ 110, 2665
Mirabel, I. F. et al., 1998, A&A 333, L1
Moorwood A. et al., 1998, The Messenger 94, 7
Neugebauer, G. & Leighton, R. B., 1969, Two-Micron Sky Survey, NASA SP-3047, Washington, D.C.
Park, O.-K., Kalnajs, A., Freeman, K. C., Koribalski, B., Staveley-Smith, L. & Malin, D. F., 2001, in ASP Conf. Ser. 230, Galaxy Disks and Disk Galaxies, eds. J. G. Funes & E. M. Corsini (San Francisco: ASP), 109
Pellerin, A., Meyer, M., Harris, J. & Calzetti, D., 2007, ApJ 658, 87
Quirk, W. J., 1972, ApJ 176, L9
Schulz, A., Henkel, C., Muders, D., Mao, R. Q., Röllig, M., & Mauersberger, R. 2007, A&A 466, 467
Schweizer, F., 2005, in ASSL, Vol. 329, Starbursts: From 30 Doradus to Lyman Break Galaxies, eds. De Grijs, R. & González Delgado, R. M. (Dordrecht: Springer), 143
Silk, J., 1997, ApJ 481, 703
Smoot, G. F., et al., 1992, ApJL 396, 1
Snijders, L., van der Werf, P. P., Brandl, B. R., Mengel, S., Schaerer, D., & Wang, Z. 2006, ApJL, 648, L25
Snijders, L., Kewley, L. J. & van der Werf, P. P., 2007, in press (arXiv:0707.1397)
Soifer, B. T., Boehmer, L., Neugebauer, G., & Sanders, D. B., 1989, AJ 98, 766
Springel, V., Frenk, C. S. & White, S. D. M., 2006, Nature 440, 1137
Stanford, S. A., Sargent, A. I., Sanders, D. B. & Scoville, N. Z., 1990, ApJ 349, 492
Tan, J. C., 2000, ApJ 536, 173
Telesco, C. M., 1988, ARA&A 26, 343
Thatte, N., Tecza, M., & Genzel, R., 2000, A&A 364, L47
Thim F., Tammann, G. A., Saha, A., Dolphin, A., Sandage, A., Tolstoy, E. & Labhardt, L., 2003, ApJ 590, 256
Toomre, A., 1964, ApJ 139, 1217
Toomre, A., 1977, in *The Evolution of Galaxies and Stellar Populations*, ed. B. M. Tinsley, & R. B. Larson (New Haven: Yale Univ. Press), 401
Tremonti, C. A., Calzetti, D., Leitherer, C. & Heckman, T. M., 2001, ApJ 555, 322
van den Bergh, S., 1980, PASP 92, 122
Vigroux, L. et al. 1996, A&A 315, L93
Wang, Z. et al. 2004, ApJ 154, 193
Weedman, D. W., Feldman, F. R., Balzano, V. A., Ramsey, L. W., Sramek, R. A. & Wu, C.-C., 1981, ApJ 248, 105
Whitmore, B. W. & Schweizer, F., 1995, AJ 109, 960
Whitmore, Bradley C. et al., 1999, AJ 118, 1551
Whitmore, B. W. & Zhang, Q., 2002, AJ 124, 1418
Whitmore, B. W. et al., 2005, AJ 130,2104
Wilson, C. D., Scoville, N., Madden, S. C.& Charmandaris, V., 2000, ApJ 542, 120
Wyse, R. F. G, 1986, ApJ 311, 41
Wyse, R. F. G & Silk, J., 1989, ApJ 339, 700
Zezas, A., Fabbiano, G., Rots, A. H., & Murray, S. S. 2002, ApJ 577, 710
Zhang, Qing, Fall, Michael F., & Whitmore, Bradley C., 2001, ApJ 561, 727